Positioning Performance Assessment of PPP-B2b Service: Static and Kinematic PPP Mode

Xiaofei Xu(✉), Zhixi Nie, Zhenjie Wang, and Yuanfan Zhang

College of Oceanography and Space Informatics, China University of Petroleum, Qingdao 266580, China
xuxiaofei.qd@gmail.com

Abstract. The whole Beidou Global Navigation Satellite System (BDS-3) constellation was completed and officially announced to provide global service on July 31, 2020. Apart from the global positioning, navigation and timing (PNT) service, BDS-3 also broadcasts real-time precise point positioning (PPP) corrections by 3 Geostationary Orbit satellites (GEOs) via PPP-B2b signal. At present, the PPP-B2b service for GPS/BDS-3 satellites is available for users in China and the surrounding area. In this paper, we conduct the PPP-B2b static and kinematic tests to evaluate the positioning performance of the BDS-3 new PPP-B2b service. Regarding PPP-B2b static positioning performance, the average positioning accuracy are 4.1 cm, 1.8 cm, and 5.2 cm in the east-, north-, and up-components, respectively. Additionally, the average horizontal and 3-dimensional positioning accuracy is about 4.5 cm and 6.9 cm. As to PPP-B2b kinematic positioning performance, the vehicle test results show that the overall positioning accuracy is 25.7 cm and 40.1 cm in horizontal and vertical components. It could be concluded that centimeter-level positioning accuracy is reached in static scenario, and decimeter-level positioning accuracy can be achieved in kinematic scenario.

Keywords: BDS-3 · GPS · PPP-B2b · Precise Point Positioning

1 Introduction

The construction of the Beidou Navigation Satellite System (BDS), which was independently developed by China, was fulfilled in 2020 [1, 2]. Beidou Global Navigation System (BDS-3) could provide global Positioning, Navigation, and Time (PNT) services. In addition, BDS-3 could also provide featured services, such as the regional/global short message service (RSMCS/GSMCS) and the satellite-based precise point positioning augmentation service (PPP-B2b) [3].

Precise Point Positioning (PPP) is a widely used GNSS positioning technology because it can reach decimeter-level or centimeter-level positioning accuracy by using a stand-along GNSS equipment [4, 5]. Motivated by the requirements of GNSS real-time application, the real-time PPP has become research hot-pot in recent years. Same as post-processing PPP, the precise satellite orbit and clock offset products are essential in real-time PPP processing [6–8]. The International GNSS Service (IGS) has launched

C. Yang and J. Xie (Eds.): *China Satellite Navigation Conference (CSNC 2022) Proceedings*, LNEE 910, pp. 241–250, 2022.
https://doi.org/10.1007/978-981-19-2576-4_21

the real-time service (RTS) in 2007. The IGS-RTS transits the precise satellite products following Networked Transport of RTCM via Internet Protocol (NTRIP), but it limited by the Internet communication [9, 10]. Afterwards, some commercial companies also launched the real-time PPP augmentation services via satellite communication. However, these services require high costs charged from users. Up to now, the BDS-3 PPP-B2b service could provide decimeter-level positioning accuracy for users in China and its surrounding areas free of charge [11]. Therefore, the PPP-B2b service, which is a great innovation of BDS, has great potential for real-time GNSS applications.

Recently, some publications have been presented concerning the assessment of the PPP-B2b corrections and the PPP-B2b positioning performance. The results indicate that the accuracy of PPP-B2b orbit products is at several decimeter-level and the standard deviation (STD) of PPP-B2b clock errors are at several centimeter-level [12, 13]. In term of PPP-B2b positioning performance, centimeter-level in static and decimeter-level in kinematic could be achieved in China and surrounding areas [14, 15]. However, most of the publications carried out the static PPP tests at permanent stations with good observation environment, such as IGS or International GNSS Monitoring and Assessment System (iGMAS) stations. As to assess the PPP-B2b kinematic positioning performance, simulated kinematic tests were conducted in most researches.

In this paper, we carry out the static and vehicle kinematic tests to assess the PPP-B2b positioning performance. At first, the precise satellite products from BDS-3 PPP-B2b messages are recovered. Then, the method of PPP-B2b real-time positioning is introduced. Finally, the static and vehicle kinematic experiments are conducted and the PPP-B2b positioning performance is analyzed.

2 Methodology

In this section, we introduce the recovery of PPP-B2b satellite orbit and clock offset products firstly. Then, the real-time PPP model using PPP-B2b service is presented.

2.1 Recovery of PPP-B2b Precise Satellite Products

In real-time PPP-B2b positioning processing, the recovery of precise satellite orbit and clock offset products is indispensable. As described in PPP-B2b Interface Control Document (ICD) [16], the PPP-B2b orbit correction parameters $\delta \boldsymbol{O}_{B2b} = \left[\delta O_{radial} \ \delta O_{along} \ \delta O_{cross} \right]^T$ are broadcasted in the radial, along-track, and the cross-track directions. But the satellites positions $\boldsymbol{X}_{brdc} = \left[X \ Y \ Z \right]^T_{brdc}$, computed by CNAV1/LNAV broadcast ephemeris, are given in the "Earth-Center Earth-Fixed" (ECEF) frame [17]. Thus, the orbit correction parameters should be transformed to the ECEF frame, this transformation can be done according to Eqs. (1)

$$\delta \boldsymbol{X}^{sat} = \left[\boldsymbol{e}_{radial} \ \boldsymbol{e}_{along} \ \boldsymbol{e}_{cross} \right] \cdot \delta \boldsymbol{O}_{B2b} \tag{1}$$

With

$$\begin{cases} \boldsymbol{e}_{radial} = \frac{\boldsymbol{r}}{|\boldsymbol{r}|} \\ \boldsymbol{e}_{cross} = \frac{\boldsymbol{r} \times \dot{\boldsymbol{r}}}{|\boldsymbol{r} \times \dot{\boldsymbol{r}}|} \\ \boldsymbol{e}_{along} = \boldsymbol{e}_{cross} \times \boldsymbol{e}_{radial} \end{cases} \tag{2}$$

where $\delta \boldsymbol{X}^{sat} = \left[\delta O_x \ \delta O_y \ \delta O_z\right]^T$ represent the PPP-B2b orbit correction vector in ECEF. $\boldsymbol{r}$ and $\dot{\boldsymbol{r}}$ are the satellite position and velocity vectors from broadcast ephemeris. It should be noted that the PPP-B2b orbit corrections for BDS-3 refer to phase center of B3 signal, and these for GPS refer to phase center of L1/L2. Then, the precise satellite positions $\left[X \ Y \ Z\right]^T_{prec,B2b}$ can be computed by:

$$\begin{bmatrix} X \\ Y \\ Z \end{bmatrix}_{prec,B2b} = \begin{bmatrix} X \\ Y \\ Z \end{bmatrix}_{brdc} - \begin{bmatrix} \delta O_x \\ \delta O_y \\ \delta O_z \end{bmatrix} \tag{3}$$

According to PPP-B2b ICD, the PPP-B2b correction parameters of satellite clock offset are relative to the clock offset from broadcast ephemeris. The precise satellite clock offsets can read as

$$dt^{sat}_{prec} = dt^{sat}_{brdc} - \frac{C_0}{c} \tag{4}$$

where dt^{sat}_{prec} and dt^{sat}_{brdc} are precise clock offset and broadcast clock offset, respectively. C_0 and c denote the PPP-B2b clock offset correction and the velocity in vacuum, respectively.

2.2 PPP Model Using PPP-B2b Service

The GNSS code and phase observations can be written as [18, 19]

$$P_i = \rho + c \cdot dt_r - c \cdot dt^s + T + \frac{f_1^2}{f_i^2} \cdot I_1 + B_{r,i} - B^s_i + \varepsilon_{P_i} \tag{5}$$

$$L_i = \rho + c \cdot dt_r - c \cdot dt^s + T - \frac{f_1^2}{f_i^2} \cdot I_1 + \lambda_i\left(N_i + b_{r,i} - b^s_i\right) + \varepsilon_{L_i} \tag{6}$$

where i represents the signal frequency; P_i and L_i are the code and phase measurements; ρ denotes the range from satellite to receiver; dt_r and dt^s are the clock offsets of receiver and satellite, respectively; f_i is the frequency value, T is the tropospheric delay, and I_1 denotes the ionospheric delay for L_i; $B_{r,i}$ and B^s_i represent the code bias at the receiver/satellite end; $b_{r,i}$ and b^s_i denote the phase bias at the receiver/satellite end; ε_{P_i} and ε_{L_i} are the unmodelled errors of code/phase measurements. It is noted that the associated empirical models should be applied to correct the other effects, such as the relativistic effect, Sagnac effect, Shapiro time delay [20], site displacements [21] and the phase windup [22], etc.

In this paper, the GNSS dual-frequency ionospheric-free (IF) combinations of code/phase observations are selected to eliminate the first-order ionospheric delay. If the receiver clock offset of ionospheric-free combinations are used as the unknown receiver clock offset, the code bias of ionospheric-free combination at the receiver end is 0, namely $B_{r,IF} = 0$. Then, the ionospheric-free combinations can be read as

$$P_{IF} = \rho + c \cdot dt_r - c \cdot dt^s - B^s_{IF} + T + \varepsilon_{P_{IF}} \tag{7}$$

$$L_{IF} = \rho + c \cdot dt_r - c \cdot dt^s + T + \lambda_{IF} \cdot \overline{N}_{IF} + \varepsilon_{L_{IF}} \tag{8}$$

where $\lambda_{IF} \cdot \overline{N}_{IF} = \lambda_{IF} N_{IF} - b^s_{IF} + b_{r,IF}$; b^s_{IF} and $b_{r,IF}$ are phase bias of ionospheric-free combination at the satellite/receiver end. λ_{IF} and N_{IF} are the ionospheric-free wavelength and the ionospheric-free ambiguity, respectively. $\varepsilon_{P_{IF}}$ and $\varepsilon_{L_{IF}}$ denote the ionospheric-free combinations noises. It should worthily be noted that the ionospheric-free code bias at the satellite need to be corrected using PPP-B2b differential code bias corrections. The PPP-B2b satellite clock offsets for BDS-3 refer to B3I signal, and these for GPS refer to L1 C/A/L2P signals. Once the recovered the PPP-B2b precise satellite products have been applied, the satellite orbit and clock errors are considered eliminated generally. Moreover, the tropospheric delay is divided into zenith dry parts and zenith wet parts. The Saastamonien model is usually used to correct the dry part, and the wet part must be estimated as unknown. After some specific errors are removed as above, the ionospheric-free combination can be linearized as:

$$p_{IF} = -\boldsymbol{e} \cdot \boldsymbol{x} + c \cdot dt_r + M_W \cdot zwd + \varepsilon_{P_{IF}} \tag{9}$$

$$l_{IF} = -\boldsymbol{e} \cdot \boldsymbol{x} + c \cdot dt_r + M_W \cdot zwd + \lambda_{IF} \cdot \overline{N}_{IF} + \varepsilon_{L_{IF}} \tag{10}$$

3 Experiments and Results Analysis

To investigate the PPP-B2b positioning performance, both the static and kinematic PPP experiments were conducted in our contribution. Two GNSS receivers are used in the field tests, one is a Femtomes FRII-PLUS receiver, and the other is a NovAtel PwrPak7 receiver. The Femtomes equipment is used to PPP-B2b messages, while the NovAtel is used as rover to collect GNSS raw observations. In static mode, the GNSS antenna were on the roof of China University of Petroleum (East China) Engineering-C building under open-sky condition. As for kinematic mode, a vehicle test was conducted and the GNSS antenna was mounted on the roof of the vehicle. The test scenarios are shown in Fig. 1, and the PPP-B2b positioning processing strategies are described in Table 1 in detail. The coordinate references were generated via Inertial Explore 8.90 (IE 8.90) software produced by NovAtel Inc.

Fig. 1. The static and kinematic PPP-B2b tests scenario

Table 1. Strategies of PPP-B2b positioning processing

Item	Models/Strategies
GNSS system	GPS and BDS-3
Signal selection	GPS: L1/L2 and BDS-3: B1C/B2a
Observables	Dual-frequency code/phase ionosphere-free combinations
Sampling rate	1 s
Observable noise	Raw code: 0.5 m in zenith direction
	Raw phase: 0.005 m in zenith direction
Weight method	Elevation dependent weight
Phase windup	Corrected
Relativistic effect	Corrected
Sagnac effect	Corrected
Shapiro time delay	Corrected
Tidal effect	Solid tide, ocean loading and pole tide were corrected according to IERS Conventions 2010
Troposphere	Zenith dry delay: corrected with Saastamoinen model, while meteorological parameters were calculated by applying global pressure and temperature (GPT) model
	Zenith wet delay: estimated for each epoch as a random walk noise with a process noise of 2 cm/sqrt(h)
	Mapping function: global mapping function (GMF)
Phase ambiguity	Estimated as a float constant for each ambiguity arc
Estimator	Kalman filter

3.1 Static Experiment Results and Analyses

Three static tests were conducted to assess the PPP performance using PPP-B2b corrections with a sampling interval of 1s. The first test (session 1) was on 04:00:00–06:59:59 of November 11, 2021, the second test (session 2) was on 02:00:00–05:59:59 of November 17, 2021, and the third test (session 3) was on 02:00:00–05:59:59 of November 18, 2021. It should be noted that the duration of each session is 3 h. The position estimates at the last epoch in each session are compared with the reference coordinates to assess the stationary positioning accuracy.

The static PPP-B2b positioning errors and the statistics of PPP-B2b positioning accuracy were illustrated in Fig. 2 and 3, respectively. As shown in figures, the PPP positioning accuracy of PPP-B2b is at centimeter-level. And the static PPP-B2b positioning performance in the up component is slightly worse than those in east/north component.

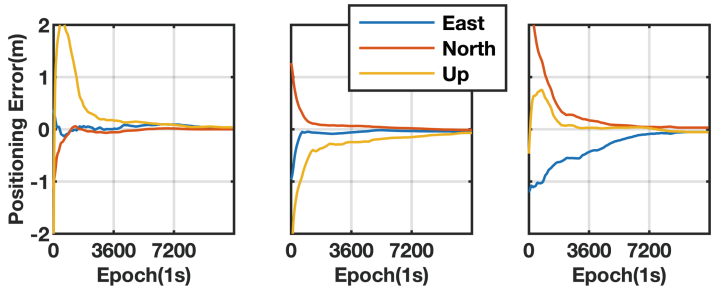

Fig. 2. Static positioning errors of PPP-B2b positioning

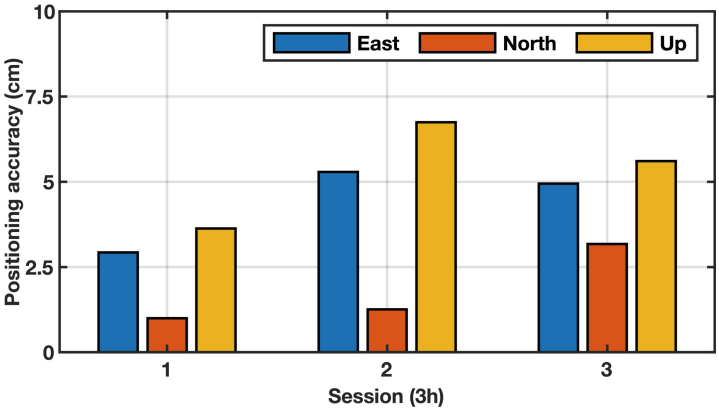

Fig. 3. Static positioning accuracy of PPP-B2b positioning

To better demonstrate the PPP-B2b positioning performance, we not only statistic the positioning accuracy in east (E)/north (N)/up (U) component, but also calculate the horizontal (H)/vertical (V)/3-dimensional (3D) positioning accuracy. For all sessions,

the positioning accuracy using PPP-B2b corrections varies by 2.5–5.1 cm in the horizontal component, and 3.5–6.5 cm in the vertical component. The detailed statistics are presented in Table 2.

Table 2. The positioning accuracy at the three sessions (unit: cm)

Session	E	N	U	H	V	3D
1	2.5	1.0	3.5	2.7	3.5	4.4
2	5.1	1.2	6.5	5.2	6.5	8.3
3	4.7	3.1	5.6	5.6	5.6	7.9

3.2 Kinematic Experiment Results and Analyses

A land vehicle kinematic test was carried out to assessing the PPP-B2b kinematic positioning performance. The environment and the trajectory of the kinematic test is shown in Fig. 4. The centimeter-level positioning solution can be solved by conducting RTK from IE 8.90 software, and this solution was applied as the reference.

Fig. 4. Vehicle test scenario and the corresponding trajectory

The duration of the vehicle test was about 20 min. The number available of BDS-3/GPS satellites and the corresponding values of PDOP and velocities is shown in Fig. 5. From the following figure, we could obtain that the average value of available satellites was 11.2, and the corresponding value of PDOP was 1.82. In terms of velocity in south-north and east-west component, most of them were within ±16 m/s.

The kinematic positioning result using PPP-B2b corrections is illustrate in Fig. 6. Generally, several decimeter-level positioning accuracies can be achieved in east/north/up direction. As can be seen from Fig. 6, a re-convergence was caused at

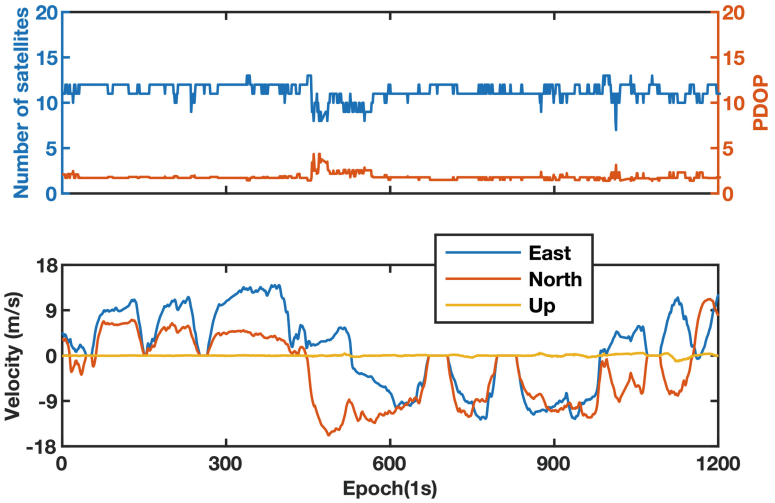

Fig. 5. Number of the available BDS-3/GPS satellites and PDOPs

around 5 min because of the outage of GNSS signal. And about 3 min was taking to achieved less than 0.6 m accuracy in vertical component at the duration of re-convergence. The overall positioning accuracy is 25.7 cm and 40.1 cm in horizontal and vertical components, respectively.

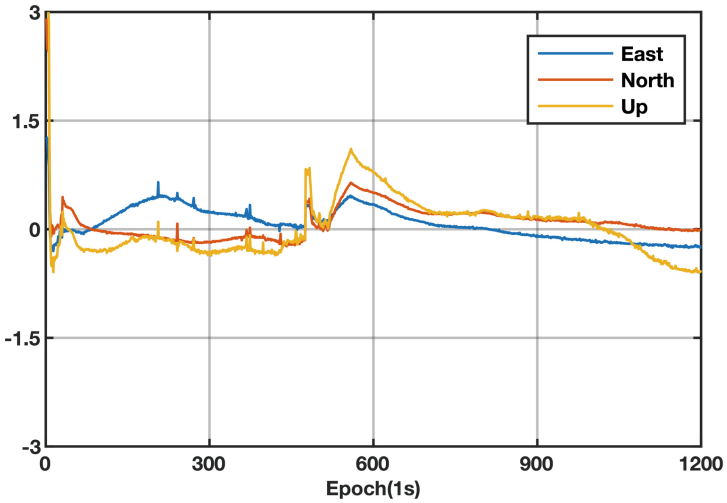

Fig. 6. Kinematic positioning errors of PPP-B2b positioning

4 Conclusions

The PPP-B2b service has started provide free PPP augmentation service to users in China and the surrounding areas since July 2020. In this paper, the assessment of PPP-B2b positioning performance, both in static and kinematic mode, was carried. Regarding PPP-B2b static positioning performance, the average positioning accuracy are 4.1 cm, 1.8 cm, and 5.2 cm in the east-, north-, and up-components, respectively. Additionally, the average horizontal and 3-dimensional positioning accuracy is about 4.5 cm and 6.9 cm. As to PPP-B2b kinematic positioning performance, the vehicle test results show that the overall positioning accuracy is 25.7 cm and 40.1 cm in horizontal and vertical components. The results of PPP tests demonstrated that the positioning accuracy could reach centimeter-level for static applications, and decimeter-level positioning accuracy could be achieved for kinematic applications.

References

1. Li, J., Yang, Y., He, H., Guo, H.: Benefits of BDS-3 B1C/B1I/B2a triple-frequency signals on precise positioning and ambiguity resolution. GPS Solutions **24**(4), 1 (2020). https://doi.org/10.1007/s10291-020-01016-8
2. Yang, Y., Mao, Y., Sun, B.: Basic performance and future developments of BeiDou global navigation satellite system. Satell. Navig. **1**(1), 1–8 (2020). https://doi.org/10.1186/s43020-019-0006-0
3. Yang, Y., et al.: Featured services and performance of BDS-3. Sci. Bull. **66**(20), 2135–2143 (2021)
4. Kouba, J., Héroux, P.: Precise point positioning using IGS orbit and clock products. GPS Solutions **5**(2), 12–28 (2001)
5. Zumberge, J., Heflin, M., Jefferson, D., Watkins, M., Webb, F.: Precise point positioning for the efficient and robust analysis of GPS data from large networks. J. Geophys. Res. Solid Earth **102**(B3), 5005–5017 (1997)
6. Li, X., Ge, M., Zhang, H., Nischan, T., Wickert, J.: The GFZ real-time GNSS precise positioning service system and its adaption for COMPASS. Adv. Space Res. **51**(6), 1008–1018 (2013)
7. Liu, T., Zhang, B., Yuan, Y., Li, M.: Real-Time Precise Point Positioning (RTPPP) with raw observations and its application in real-time regional ionospheric VTEC modeling. J. Geodesy **92**(11), 1267–1283 (2018). https://doi.org/10.1007/s00190-018-1118-2
8. Nie, Z., Yang, H., Zhou, P., Gao, Y., Wang, Z.: Quality assessment of CNES real-time ionospheric products. GPS Solutions **23**(1), 1–15 (2018). https://doi.org/10.1007/s10291-018-0802-2
9. Hadas, T., Bosy, J.: IGS RTS precise orbits and clocks verification and quality degradation over time. GPS Solutions **19**(1), 93–105 (2014). https://doi.org/10.1007/s10291-014-0369-5
10. Nie, Z., Gao, Y., Wang, Z., Ji, S., Yang, H.: An approach to GPS clock prediction for real-time PPP during outages of RTS stream. GPS Solutions **22**(1), 1–14 (2017). https://doi.org/10.1007/s10291-017-0681-y
11. Liu, C., et al.: Design and implementation of a BDS precise point positioning service. Navig. J. Inst. Navig. **67**(4), 875–891 (2020)
12. Tao, J., Liu, J., Hu, Z., Zhao, Q., Chen, G., Ju, B.: Initial Assessment of the BDS-3 PPP-B2b RTS compared with the CNES RTS. GPS Solutions **25**(4), 1–16 (2021). https://doi.org/10.1007/s10291-021-01168-1

13. Xu, Y., Yang, Y., Li, J.: Performance evaluation of BDS-3 PPP-B2b precise point positioning service. GPS Solutions **25**(4), 1–14 (2021). https://doi.org/10.1007/s10291-021-01175-2
14. Nie, Z., Xu, X., Wang, Z., Du, J.: Initial assessment of BDS PPP-B2b service: precision of orbit and clock corrections, and PPP performance. Remote Sens. **13**(11), 2050 (2021)
15. Zhang, W., Lou, Y., Song, W., Sun, W., Zou, X., Gong, X.: Initial assessment of BDS-3 precise point positioning service on GEO B2b signal. Adv. Space Res. **69**(1), 690–700 (2022)
16. China Satellite Navigation Office (CSNO): BeiDou Navigation Satellite System Signal In Space Interface Control Document Precise Point Positioning Service Signal PPP-B2b (Version 1.0). http://www.beidou.gov.cn/xt/gfxz/202008/P020200803362062482940.pdf. Assessed 9 Dec 2020
17. Montenbruck, O., Steigenberger, P., Hauschild, A.: Broadcast versus precise ephemerides: a multi-GNSS perspective. GPS Solutions **19**(2), 321–333 (2014). https://doi.org/10.1007/s10291-014-0390-8
18. Leick, A., Rapoport, L., Tatarnikov, D.: GPS Satellite Surveying. Wiley, New York (2015)
19. Xu, G., Xu, Y.: GPS: Theory, Algorithms and Applications. Springer, Berlin (2016). https://doi.org/10.1007/978-3-662-50367-6
20. Ashby, N.: Relativity in the global positioning system. Living Rev. Relativ. **6**(1), 1–42 (2003). https://doi.org/10.12942/lrr-2003-1
21. Petit, G., Luzum, B.: IERS conventions (2010). Bureau International Des Poids et Mesures Sevres:Frankfurt am Main, Germany (2010)
22. Wu, J.-T., Wu, S.C., Hajj, G.A., Bertiger, W.I., Lichten, S.M.: Effects of antenna orientation on GPS carrier phase. Astrodynamics **1992**, 1647–1660 (1991)